JOURNAL OF GEOPHYSICAL RESEARCH, VOL. 111, D21116, doi:10.1029/2005JD006821, 2006

Click Here for Full Article

Seasonally varying modes in long-term variability of European precipitation during the 20th century

Igor I. Zveryaev[1]

Received 26 October 2005; revised 23 July 2006; accepted 24 July 2006; published 14 November 2006.

[1] A gridded monthly terrestrial gauge-based precipitation for 1901–2000 from the Climatic Research Unit, University of East Anglia, set is used to investigate leading seasonal modes in the long-term precipitation variability over Europe and their links to atmospheric circulation. Performed empirical orthogonal function (EOF) analysis has shown that the leading modes of precipitation variability over Europe are clearly season-dependent. The character of the links between regional precipitation and atmospheric circulation also features essential seasonality. The first EOF modes of the winter, spring, and summer seasonal mean precipitation over Europe are associated with the North Atlantic Oscillation (NAO). However, because the summer NAO differs significantly from the winter and spring NAO, the first EOF mode of the summer precipitation has a spatial-temporal structure which is principally different from those of the winter and spring seasons. The first EOF mode of the fall precipitation is not associated with the NAO. This mode demonstrates a strong link to the Scandinavian teleconnection pattern. The second EOF modes of the winter and fall precipitation are linked to the east Atlantic and the NAO teleconnection patterns, respectively. Analysis of running correlations between the principal components of the leading EOF modes of precipitation and the NAO index has revealed nonstationarity of the links between European precipitation and the NAO. Moreover, there is evident seasonality in the character of the long-term changes of the above links.

Citation: Zveryaev, I. I. (2006), Seasonally varying modes in long-term variability of European precipitation during the 20th century, *J. Geophys. Res.*, *111*, D21116, doi:10.1029/2005JD006821.

1. Introduction

[2] Precipitation is one of the key climatic parameters whose variability influences a wide range of human activities. Both deficient and excessive precipitation may cause serious social and economic consequences. This is especially true for the densely populated regions where the consequences might be catastrophic. Certainly Europe is one of such regions. In recent years there were many examples of extremely low/high precipitation in different parts of Europe that resulted in significant damage to the regional economies [e.g., *Christensen and Christensen*, 2003; *Zveryaev*, 2004].

[3] The majority of the climate variability studies in the Atlantic-European sector were focused on the cold season [e.g., *Wibig*, 1999; *Rodwell et al.*, 1999; *Zveryaev*, 1999; *Cassou and Terray*, 2001; *Slonosky et al.*, 2001; *Drevillon et al.*, 2001]. Because winter months are dynamically the most active, perturbations in the atmospheric circulation can grow to large amplitudes. Thus interest in the winter climate variability is understandable. Less attention has been given to European climate variability during other seasons [*Colman and Davey*, 1999; *Hurrell and Folland*, 2002; *Zveryaev*, 2004], and to the seasonality [*Shabalova and Weber*, 1998; *Portis et al.*, 2001; *Zolina et al.*, 2005] of climate variations in the Atlantic-European sector. However, climate anomalies during other seasons are not of less importance than those during winter season. Therefore, to improve regional climate modeling and prediction, further analysis of the European climate variability during all seasons is necessary.

[4] During recent years a number of papers were focused on the variability and changes in precipitation over Europe [e.g., *Zorita et al.*, 1992; *von Storch et al.*, 1993; *Hurrell*, 1995; *Wibig*, 1999; *Corte-Real et al.*, 1998; *Qian et al.*, 2000]. Most of these studies were based on the analysis of winter or annual mean precipitation. Recently, using relatively short time series of satellite-derived precipitation data [*Xie and Arkin*, 1996, 1997], we analyzed and compared intraseasonal and interannual variability of European precipitation during winter and summer seasons [*Zveryaev*, 2004]. Evident seasonal differences have been revealed in all considered characteristics of precipitation variability. The present study expands and complements in many respects our previous analysis. First, century-long time series of precipitation used in this study allow analysis of not only interannual but also decadal-interdecadal variations. Secondly, we expand our analysis to all seasons (including spring and fall). Thirdly, applying running window correlation analysis we investigate long-term evolution of the strength of links between the leading modes of European precipitation and

[1]P. P. Shirshov Institute of Oceanology, Russian Academy of Sciences, Moscow, Russia.

Copyright 2006 by the American Geophysical Union.
0148-0227/06/2005JD006821$09.00

the North Atlantic Oscillation (hereafter NAO) during the 20th century. Though observational data analysis alone may not be able to disclose the cause and effect relationship between different components of the climate system, understanding of the observational links enhances ability for seasonal predictions of the European climate.

[5] In the present study we focus on the analysis of the winter, spring, summer and fall precipitation variability over Europe on timescales from interannual to interdecadal, and on the links between this variability and regimes of the atmospheric circulation. We analyze long-term variability of precipitation over Europe on the basis of relatively continuous in time and spatially homogeneous data of precipitation available from the Climatic Research Unit, University of East Anglia (CRU) [*New et al.*, 1999, 2000; *Mitchell and Jones*, 2005] data set. Special emphasis is made on the seasonal differences in precipitation variability. The paper is organized as follows. The data used and analysis methods are described in section 2. Spatial-temporal structure of the leading modes of the seasonal mean precipitation variability for each season for 1901–2000 is analyzed in section 3. Links between leading modes of precipitation variability and atmospheric circulation and teleconnection patterns are examined in section 4. Finally, a summary and discussion are presented in section 5.

2. Data and Methods

[6] In the present study we used the CRU TS 2.0 0.5° latitude-longitude gridded monthly precipitation data [*Mitchell and Jones*, 2005] which is a revised and extended version of the earlier constructed data set [*New et al.*, 1999, 2000]. This data set has been constructed at the Climatic Research Unit (CRU), University of East Anglia. The data set presents terrestrial surface climate for the 1901–2000 period. This data set has higher spatial resolution than other data sets of similar temporal extent, and it has longer temporal coverage than other products of similar spatial resolution. The precipitation data for the European region used in this study were interpolated directly from station observations. Details on data construction method can be found in work by *Mitchell and Jones* [2005]. It is worth noting that intercomparison of these data with satellite-based precipitation data from the Climate Prediction Center Merged Analysis of Precipitation (CMAP) data set [*Xie and Arkin*, 1996, 1997] showed a good agreement between the two data sets both in terms of climatologies and leading modes of precipitation variability [*Zveryaev*, 2004]. In the present study the domain of analysis is limited to latitudes 34°N–71°N and longitudes 11°W–50°E. Since we analyze seasonal mean precipitation (not seasonal precipitation totals) expressed in mm/month, it would be correct to use term "precipitation rate". However, for the sake of shortness, further in the text we use term "precipitation". Moreover, we neither show no discuss real values of precipitation. Rather, we are focused on characteristics of precipitation variability and links to atmospheric circulation.

[7] To assess the links between variability of European precipitation and major climatic signal in the region, the NAO, we use the principal component based on NAO indices provided by the Climate Analysis Section, NCAR, Boulder, USA, *Hurrell* [1995]. The leading eigenvectors of the cross-covariance matrix were calculated for each season from the seasonal sea level pressure anomalies in the North Atlantic–European sector (20°–80°N; 90°W–40°E). These data are available from the Web site http://www.cgd.ucar.edu/~jhurrell/nao.pc.html.

[8] We also use the major teleconnection patterns indices that have been documented and described by *Barnston and Livezey* [1987]. These regularly updated indices are available from the Climate Prediction Center (CPC) website http://www.cpc.ncep.noaa.gov/data/teledoc/telecontents.shtml. The data cover the period 1950– present. Details on the teleconnection pattern calculation procedures can be found in the work by *Barnston and Livezey* [1987] and at the CPC website.

[9] To reveal dynamical context of the leading modes in precipitation variability, we have used Met Office–Northern Hemisphere Mean Sea Level Pressure Data [*Basnett and Parker*, 1997] provided by the British Atmospheric Data Centre. This data set holds gridded (5° latitude by 10° longitude grid) Northern Hemisphere (north of 15°N) monthly and daily series of mean sea level pressure (MSLP) fields. The monthly series data are available for the period 1873–present. In the present study we use data for 1901–2000. For the same purpose, as a complimentary data set, we use monthly 500 hPa geopotential heights data from the NCEP/NCAR Reanalysis for 1951–2000 [*Kalnay et al.*, 1996]. These data have a 2.5° latitude by 2.5° longitude spatial resolution.

[10] We examine a spatial-temporal structure of the long-term variations of seasonal mean precipitation over Europe by application of empirical orthogonal functions (EOF) analysis on the basis of the covariance matrix [*Wilks*, 1995; *von Storch and Navarra*, 1995]. Prior to the EOF analysis the annual cycle was removed from all grid point time series by subtracting from each seasonal value the respective season's long-term mean. In order to take into account the latitudinal distortions, obtained anomalies were weighted by the square root of cosine of latitude to ensure that equal areas are afforded equal weight in the analysis [*North et al.*, 1982]. The long-term stationarity of the time series is preserved for the calculation of EOF through detrending the time series with a linear least squares fit. To validate results, we applied EOF analysis to normalized time series of precipitation. Only robust modes of precipitation variability that were evident both in original and normalized time series are considered in the paper.

[11] To assess links to teleconnection patterns we use conventional correlation analysis. No lead or lag relationships were taken into consideration for this work; our analysis was restricted to simultaneous connections between seasonal precipitation variability over Europe and major teleconnection patterns and SLP and 500 hPa fields in the North Atlantic–European sector. According to Student's *t* test [*Bendat and Piersol*, 1966], the minimum significant correlation coefficients between the time series analyzed are 0.195 (0.277 for 50-year time series) and 0.256 (0.358) for the 95% and 99% significance levels, respectively. To investigate long-term variations in the strength of links between European precipitation and the NAO, we also performed an analysis of running correlations. Analysis of running correlations is widely used to investigate stability of the links between different climatic parameters. For example, *Pauling*

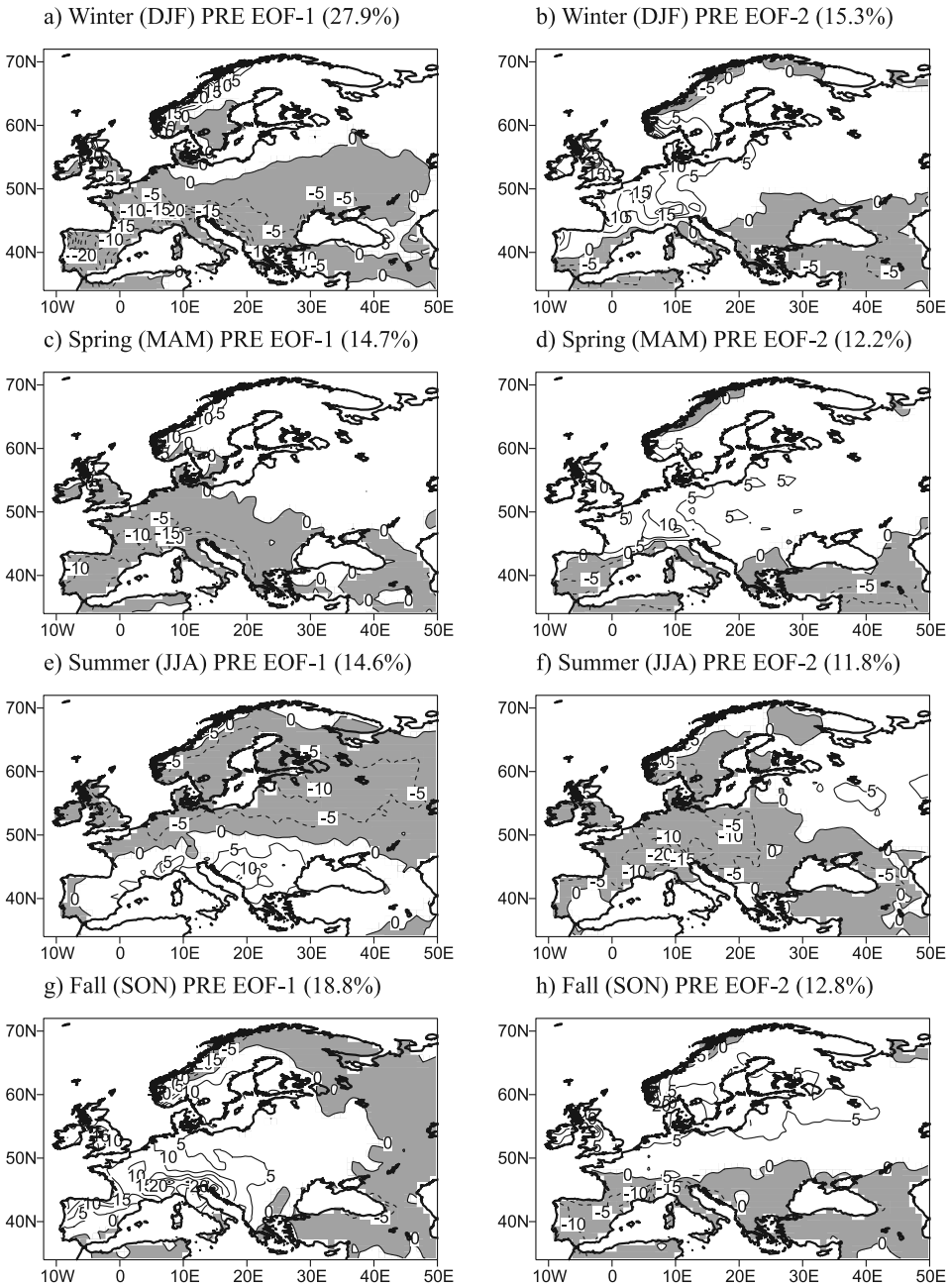

Figure 1. Spatial patterns of the first two EOF modes of the (a, b) winter, (c, d) spring, (e, f) summer, and (g, h) fall CRU precipitation (1901–2000). Units are mm/month. Dashed curves and shadings indicate negative values.

et al. [2006] applied running correlations in their study of the relationships between large-scale atmospheric circulation and regional precipitation over southern Spain and central Europe. Earlier *Slonosky et al.* [2001] used similar approach to investigate long-term changes in the links between atmospheric circulation and surface temperature in Europe. It is worth noting that the significance level of the correlation coefficient might be reduced if the time series are influenced by autocorrelation. Briefly, large lag-one autocorrelations reduce significantly effective number of degrees of freedom, while influence of small autocorrelations is weak [e.g., *Bretherton et al.*, 1999]. We have examined the potential impact of autocorrelation on the estimation of significance of correlation coefficients (estimated through the Fisher z transform). Neither time series (i.e., principal components of the leading EOF modes) considered in the study revealed significant autocorrelations.

3. Leading Modes of the Seasonal Mean Precipitation Variability

[12] To reveal and analyze leading modes of long-term variability of precipitation over Europe during the 20th century, we performed the EOF analysis on time series of the winter, spring, summer, and fall seasonal mean precipitation from the CRU data set for the period 1901–2000.

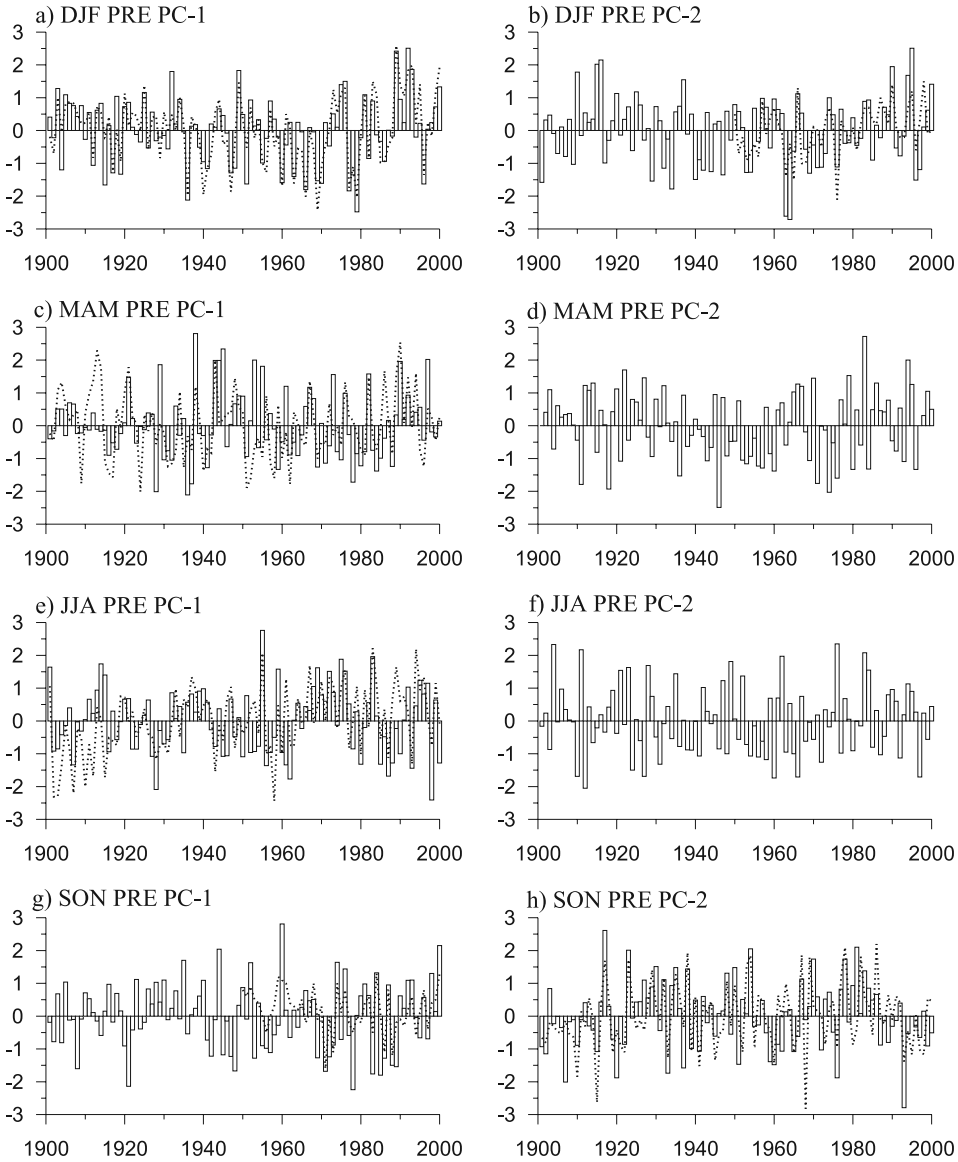

Figure 2. Principal components of the first two EOF modes of the (a, b) winter, (c, d) spring, (e, f) summer, and (g, h) fall CRU precipitation (1901–2000). Dotted curves depict the NAO index in Figures 2a, 2c, 2e, and 2h; the EA index in Figure 2b; and the SCA index in Figure 2g.

We limit our analysis to consideration of the first and second EOF modes, because each of the subsequent modes explains less than 10% of the total precipitation variance in any season, and because significant links between those modes of precipitation variability and regimes of atmospheric circulation were not found. Spatial patterns of the first two EOF modes of precipitation and time series of the corresponding principal components (hereafter PC) are shown, respectively, in Figures 1 and 2.

[13] The first EOF mode explains 27.9% of the total variance of winter precipitation. The respective spatial pattern (Figure 1a) shows two major action centers of opposite polarity with the largest loadings over northwestern Scandinavia and the Mediterranean region. The pattern reflects opposite DJF precipitation variations over northern and southern Europe. Structurally the obtained pattern is very similar to that of the first EOF mode of the winter precipitation from the CMAP data for 1979–2001 [*Zveryaev*, 2004]. The explained variance, however, is essentially lower than that obtained from analysis of CMAP precipitation (42.1%). In general, that suggests the relative role of the first EOF mode in winter precipitation variability changed significantly during the 20th century, and that this mode was better pronounced during recent decades. It is worth noting, however, that the other factors (e.g., different spatial resolution, coverage of marine/oceanic regions by the CMAP data, etc.) might also partly explain the above difference. Nevertheless, it is more likely that the first EOF mode of winter precipitation was indeed better pronounced during recent decades since our estimates based on the CRU data for 1958–1998 showed that this mode accounted for 30.2% of the winter precipitation variance during that period [*Zveryaev*, 2004]. To investigate further this subject, we performed separate EOF analysis for the two climatic periods (1901–1978 and 1979–2000),

Table 1. Fractions of the Total Winter Precipitation Variances, Explained by the First and Second EOF Modes

	EOF-1, %	EOF-2, %
Winter PRE 1901–2000	27.9	15.3
Winter PRE 1901–1978	25.7	15.2
Winter PRE 1979–2000	38.4	16.4

basing on the CRU data that are not effected by satellite observations. As seen from Table 1, contribution of the first EOF mode to the winter precipitation variability changed from 25.7% in 1901–1978 to 38.4% in 1979–2000. Thus the relative role of this mode in total variability of winter precipitation indeed significantly increased during recent decades. The PC1 (Figure 2a), displaying temporal behavior of this mode, features an upward trend during recent decades. This trend is consistent with the earlier described positive trend of the NAO index [e.g., *Hurrell*, 1995]. To clarify usage of term "trend" in analysis of time series in Figure 2, we note that we mean trends of principal components that are not the trends of real precipitation. Depending on the sign (positive or negative) of the values of the respective spatial pattern, positive (for example) trend of PCs may reflect both increase and decrease of precipitation.

[14] The second EOF mode accounts for 15.3% of the total variance of DJF precipitation. The respective spatial pattern (Figure 1b) depicts three action centers. The pattern reflects coherent precipitation variations over the Mediterranean and Black Sea region and northwestern Scandinavia, and opposite variations over the rest part of Europe with remarkably large loadings over western and central Europe. As in the case of the first EOF mode, this pattern is also similar to that of the second EOF mode of the winter CMAP precipitation [*Zveryaev*, 2004]. The PC2 displays long-term interdecadal variations characterized by a downward trend from the late 1910s to the early 1960s that changed to an upward trend during the later period (Figure 2b). Earlier multidecadal variability of the NAO index with its fall to the 1960s and a rise into the 1990s has been revealed [e.g., *Rodwell and Folland*, 2002]. However, since the recent upward trend in Figure 2b starts somewhat earlier than the positive trend of the NAO index [*Hurrell*, 1995], it cannot be a result of the NAO strengthening and respective increase in zonal moisture transport to European region. For the same reason, the upward trend of the PC2 is unlikely to be associated with the recent intensification of the global warming expressed by the strong positive trend of the global and hemispheric surface temperatures that started in the late 1970s [e.g., *Parker et al.*, 1994; *Jones and Moberg*, 2003]. Although the second EOF mode explains relatively low percentage of winter precipitation variance, the local effect of this mode might be essential in the regions characterized by the large loadings (e.g., central Europe).

[15] During spring the first EOF mode accounts for 14.7% of the total variance of precipitation. This is almost half of the fraction of variance explained by the first EOF mode of winter precipitation (27.9%). Differing in some details, the respective spatial pattern (Figure 1c) is similar to that of the first EOF mode of DJF precipitation (Figure 1a) and displays two major action centers of opposite polarity over northwestern Scandinavia and the Mediterranean region, that reflect opposite MAM precipitation variations over northern and southern Europe. Despite some similarities (such as predominantly positive anomalies during the last decade) interannual behavior of this mode, depicted by the PC1 (Figure 2c), differs from that of the first EOF mode of winter precipitation and correlation between the respective time series is low (0.23).

[16] The second EOF mode explains 12.2% of the total variance of MAM precipitation. Its spatial pattern (Figure 1d) is structurally similar to that of the second EOF mode of winter precipitation (Figure 1b), and reflects coherent precipitation variations over the Mediterranean region and northwestern Scandinavia, and opposite variations over the rest part of Europe. Temporal behavior of the PC2 is characterized by long-term trend-like changes (Figure 2d). Like in the case of the first EOF mode, PC of this mode is not correlated to that of the second EOF mode of winter precipitation.

[17] During summer the first EOF mode explains 14.6% of the total variance of precipitation. The spatial pattern depicts three action centers: over the southern Europe/Mediterranean and Black Sea region, a large portion of Europe north of approximately 48°N, and a minor center over northeastern Scandinavia (Figure 1e). While the variation of JJA precipitation over the southern Europe/Mediterranean and Black Sea region and northeastern Scandinavia is in phase, it is opposite to that over a large portion of Europe between 48°N and 68°N. Structurally this pattern is principally different from those of the first EOF modes of winter (Figure 1a) and spring (Figure 1c) precipitation. Like the pattern of the first EOF mode of winter precipitation, this pattern is similar to that of the first EOF mode of the summer CMAP precipitation [*Zveryaev*, 2004]. PC of this mode (Figure 2e) demonstrates decadal-scale variations characterized by multiyear periods of positive and negative anomalies. Earlier we noted [*Zveryaev*, 2004] that this feature of decadal-scale variability has been revealed by *Hurrell and Folland* [2002] in summer (July August) time series of sea level pressure over northeast Atlantic.

[18] The second EOF mode of summer precipitation accounts for 11.8% of its total variance. The spatial pattern of this mode (Figure 1f) is characterized by the coherent precipitation variations over large portion of European Russia, part of Scandinavia and some Mediterranean regions and opposite variations over the remaining part of Europe. Consistent with the results of analysis of the CMAP precipitation [*Zveryaev*, 2004], a very weak third anomaly center is detected over southern Italy and the Balkans, where variations of precipitation are synchronized with those over European Russia and part of Scandinavia. Compared to the first EOF mode (Figure 2e), the PC2 displays shorter-term variability of precipitation (Figure 2f).

[19] During fall the first EOF mode accounts for 18.8% of the total variance of precipitation. The spatial pattern of this mode (Figure 1g) shows coherent precipitation variations over the eastern part of European Russia and northern and eastern Scandinavia (with the largest loadings over northern Scandinavia), and opposite variations of SON precipitation over the remaining part of Europe (with the largest loadings over central Europe and the Adriatic region). The pattern is noticeably different from those obtained for the first EOF modes of precipitation variability during other seasons (Figures 1a, 2c, and 2e). The PC1 (Figure 2g) demonstrates the

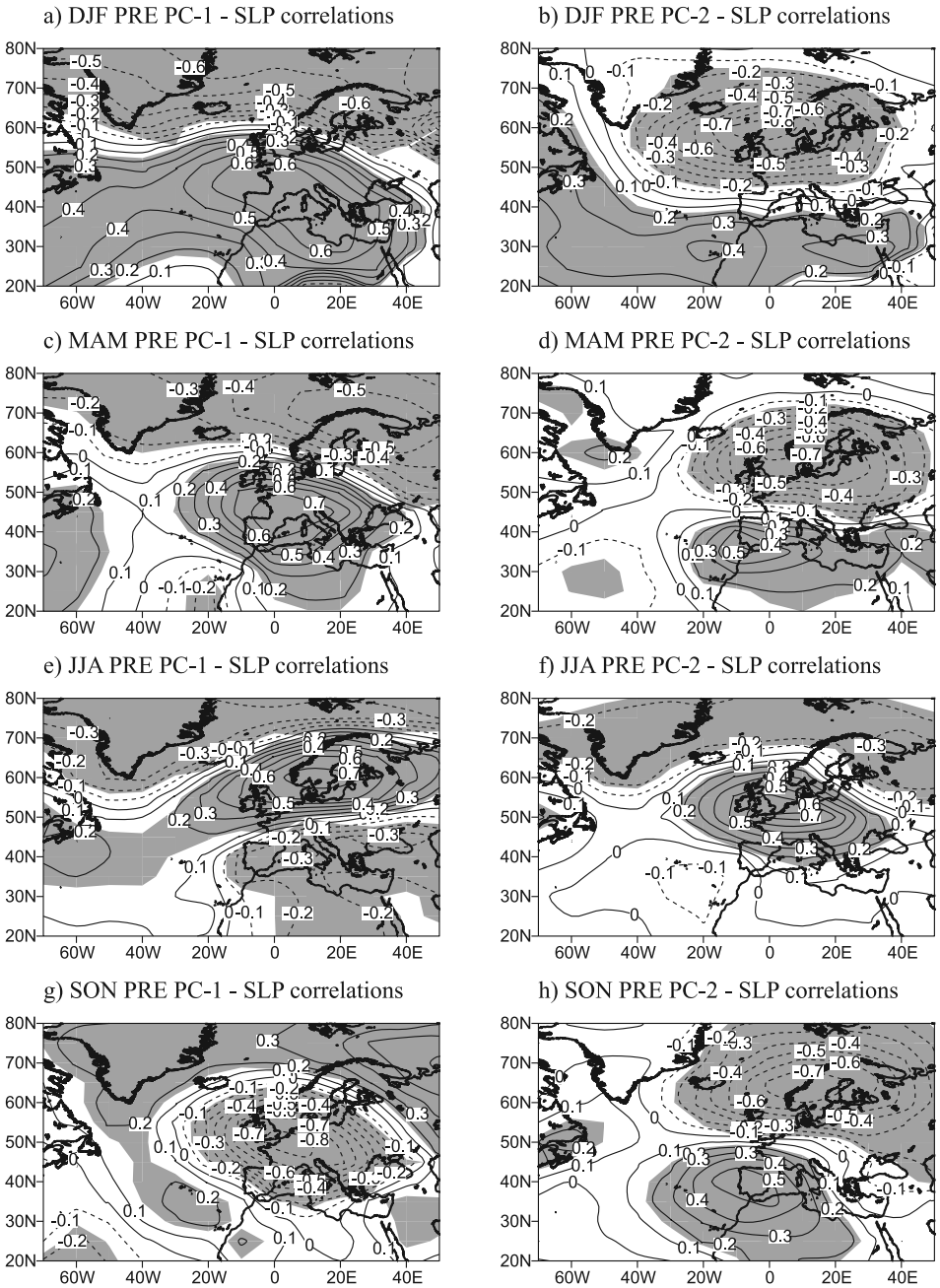

Figure 3. Correlation coefficients between principal components of the first two EOF modes of the (a, b) winter, (c, d) spring, (e, f) summer, and (g, h) fall CRU precipitation (1901–2000) and respective SLP fields. Shaded areas indicate the 95% significance level.

temporal behavior of this mode, characterized by the evident upward trend persisted from late 1970s until the end of the century. However, in contrast to other seasons the first EOF mode of SON precipitation is not associated with the NAO. Correlation between the PC1 and the fall NAO index is very low (0.1) and statistically insignificant. It is also seen (Figure 2g) that the recent positive trend revealed in the winter NAO index, is not present in the fall NAO index.

[20] The second EOF mode explains 12.8% of the total variance of SON precipitation. Though the loadings over Iberian peninsula and western Scandinavia are not as large, structurally, the spatial pattern (Figure 1h) of this mode is similar to those of the first EOF modes of winter and spring precipitation (Figures 1a and 1c) reflecting opposite precipitation variations over northern and southern Europe. Notably, the PC2 demonstrates downward (i.e., opposite to that of the first EOF mode) trend during last two decades of the 20th century (Figure 2h).

[21] Summarizing results of this section, we note that the analyzed leading EOF modes of European precipitation are clearly season-dependent. While the first EOF modes of the winter, spring and summer precipitation are all associated with the NAO, the summer mode is principally different (in terms of spatial-temporal structure) from winter and spring

Table 2. Correlation Coefficients Between Principal Components of the First and Second EOF Modes of Seasonal Mean Precipitation and Indices of Teleconnection Patterns[a]

	PC-1	PC-2
	Winter	
NAO_W	0.85	
EA_W		0.61
	Spring	
NAO_{SP}	0.41	
	Summer	
NAO_S	0.50	
	Fall	
NAO_F		0.57
SCA	0.69	

[a]Shown coefficients are statistically significant at the 99% significance level.

ones. Moreover, the first EOF mode of the fall precipitation is not associated with the NAO.

4. Links to Atmospheric Circulation

4.1. Correlations With SLP and 500 hPa Fields

[22] To examine links between precipitation variability and atmospheric circulation we consider the correlations between PCs of the leading modes of seasonal mean precipitation and seasonally averaged SLP fields for 1901–2000. The domain of correlation analysis is North Atlantic–European sector limited to latitudes 20°N–80°N and longitudes 70°W–50°E. Results of the correlation analysis are shown in Figure 3, in which positive (negative) correlations are depicted by solid (dashed) curves, and significance level exceeding 95% is indicated by shading.

[23] Figure 3a shows correlations between PCs of the first EOF mode of winter precipitation and seasonally averaged winter SLP. The correlations form a meridional dipole pattern with the largest negative correlations (−0.6) over northern part of the analysis domain, and the largest positive correlations (0.6) over the western Europe–Mediterranean region. Indeed, the obtained pattern is typical for the positive phase of NAO that is characterized by below normal SLP in the region around Iceland, and above normal SLP in the extensive region around Azores. This results in excessive (deficient) precipitation over northern (southern) Europe [e.g., *Hurrell*, 1995; *Zveryaev*, 2004]. Correlation between the PC1 and the winter NAO index (see Table 2) is very high (0.85) and statistically significant at the 99% confidence level according to Student's *t* test [*Bendat and Piersol*, 1966]. Thus, consistent with earlier studies [e.g., *Hurrell*, 1995; *Zveryaev*, 2004], our correlation analysis shows that the first EOF mode of winter precipitation over Europe is linked to the major climatic signal in the region: the NAO.

[24] Correlations between PC of the second EOF mode of winter precipitation and seasonally averaged DJF SLP are depicted in Figure 3b. The pattern represents dipole with two action centers of opposite polarity. The largest negative correlations (−0.8) are found over the North Sea, and the largest positive correlations (0.4) are detected over eastern tropical Atlantic. We note that the second action center is essentially weaker than the first one. Though there is some similarity between this pattern and the correlation pattern considered in the previous paragraph, there is also an apparent difference. Besides previously noted difference in the strength of two action centers, the dipole is shifted significantly southward compared to that in Figure 3a. The second EOF mode of DJF precipitation over Europe is associated with the east Atlantic (hereafter EA) teleconnection pattern (correlation between respective time series is 0.61) having some structural similarity to the NAO [*Barnston and Livezey*, 1987].

[25] Figure 3c depicts correlations between PC of the first EOF mode of spring precipitation and seasonally averaged spring SLP. The correlations form a southwest-northeast oriented dipole with the largest negative correlations (−0.5) over eastern Scandinavia, and the largest positive correlations (reaching 0.7) over western Europe. Though the pattern is somewhat similar to the one obtained for the first EOF mode of winter precipitation (Figure 3a), the northern center of largest negative correlations is shifted eastward, and both centers are more localized compared to those in Figure 3a. As seen from Table 2, correlation between the PC1 and the spring NAO index is moderately high (0.41) and statistically significant at the 99% significance level according to Student's *t* test [*Bendat and Piersol*, 1966]. However, the link to the NAO is essentially weaker than that during winter season (0.85).

[26] Correlations between PC of the second EOF mode of spring precipitation and seasonally averaged MAM SLP are shown in Figure 3d. The pattern is characterized by a meridional dipole located in the eastern part of the domain of analysis. The largest negative correlations (−0.7) are detected over southwestern Scandinavia, and the largest positive correlations (0.5) are found over southwestern Europe and northwestern Africa. In general, the pattern is similar to a structure illustrating positive phase of the NAO, but displaced southeastward. However, the PC2 of spring precipitation does not show significant correlation to the spring NAO index. Correlation analysis also did not reveal significant links between this mode of MAM precipitation variability over Europe and other regional teleconnection patterns.

[27] Figure 3e displays correlations between PC of the first EOF mode of summer precipitation and seasonally averaged summer SLP. The correlations form a meridional tripole pattern with the largest positive correlations (0.7) over northern Europe, and negative correlations north and south of this region. The correlation pattern in Figure 3e is very similar to the NAO pattern for the summer season obtained by *Barnston and Livezey* [1987]. The obtained correlation pattern implies that above normal SLP (i.e., anticyclonic anomaly) over Baltic region results in deficient precipitation, whereas negative SLP anomalies north and south of this region are associated with excessive precipitation over northern Scandinavia and southern Europe (Figure 1e). Though the spatial-temporal structure of the first EOF mode of JJA precipitation differs significantly from those of the first EOF modes of winter and spring precipitation, correlation analysis suggests an association of this mode with the summertime NAO (correlation between the PC1 and the summer NAO index is 0.50).

[28] Correlations between PC of the second EOF mode of summer precipitation and seasonally averaged JJA SLP are

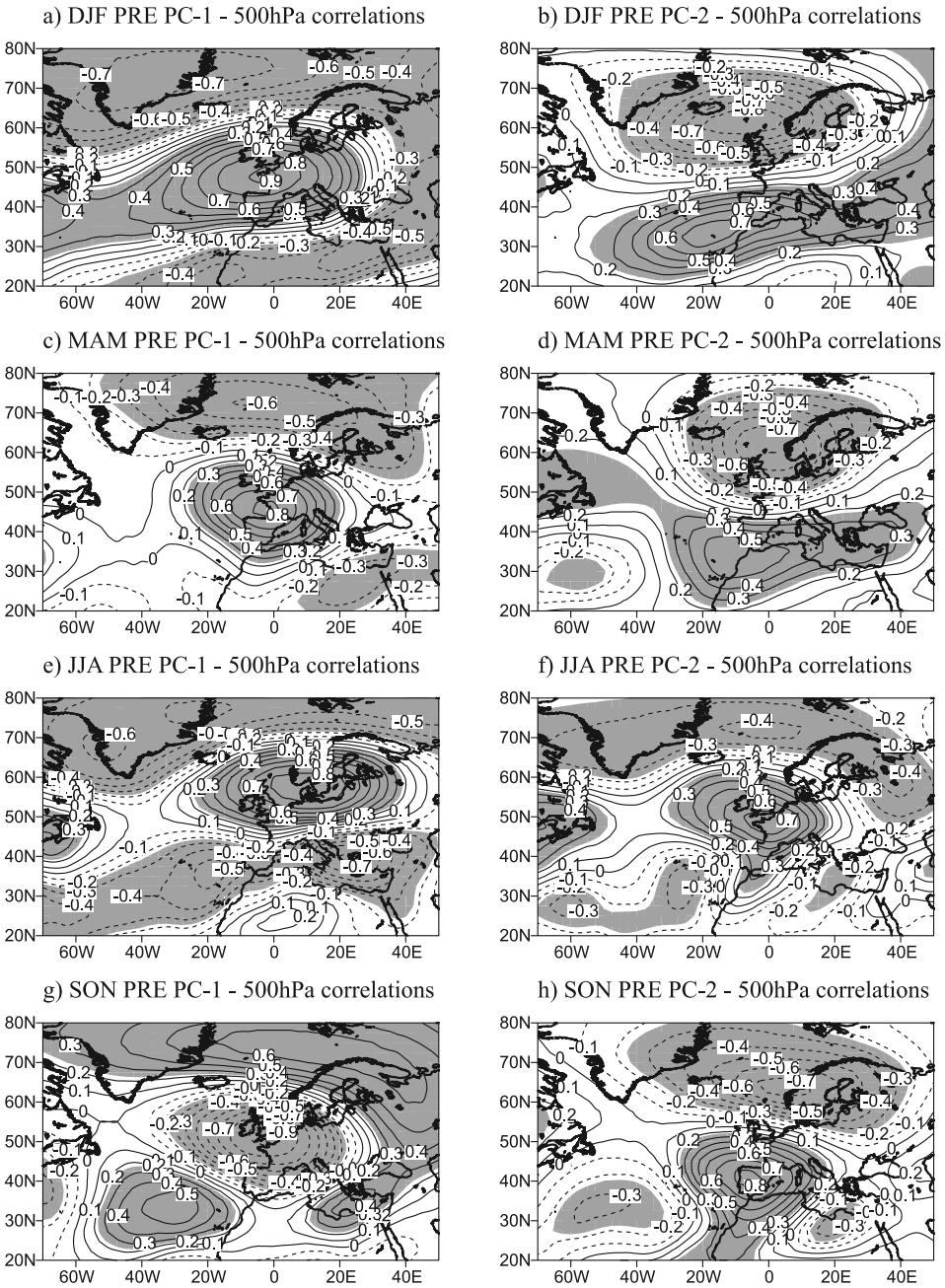

Figure 4. Correlation coefficients between principal components of the first two EOF modes of the (a, b) winter, (c, d) spring, (e, f) summer, and (g, h) fall CRU precipitation (1951–2000) and respective 500 hPa fields. Shaded areas indicate the 95% significance level.

depicted in Figure 3f. The pattern shows major center of positive correlations (reaching 0.7) centered over central western Europe and the British Isles. This action center implies that positive (negative) SLP anomalies result in below (above) normal precipitation in the region (Figure 1f). Significant negative correlations seen in the northern part of the region are essentially weaker (−0.2–0.3). Correlation analysis did not reveal significant links between the second EOF mode of summer precipitation and regional teleconnection patterns.

[29] Figure 3g shows correlations between PC of the first EOF mode of fall precipitation and seasonally averaged fall SLP. In general, the pattern is similar to the correlation pattern obtained for the second EOF mode of summer precipitation (Figure 3f), but the signs of correlations are reversed. The pattern shows a major center of negative correlations (reaching −0.8) centered over central western Europe and the British Isles. Significant positive correlations detected around this center are essentially lower. The PC1 is strongly correlated (0.69) with index of the Scandinavian teleconnection pattern (hereafter SCA), suggesting that the first EOF mode of fall precipitation is associated with this mode of atmospheric circulation. The correlation pattern in Figure 3g is also structurally similar to the fall SCA teleconnection

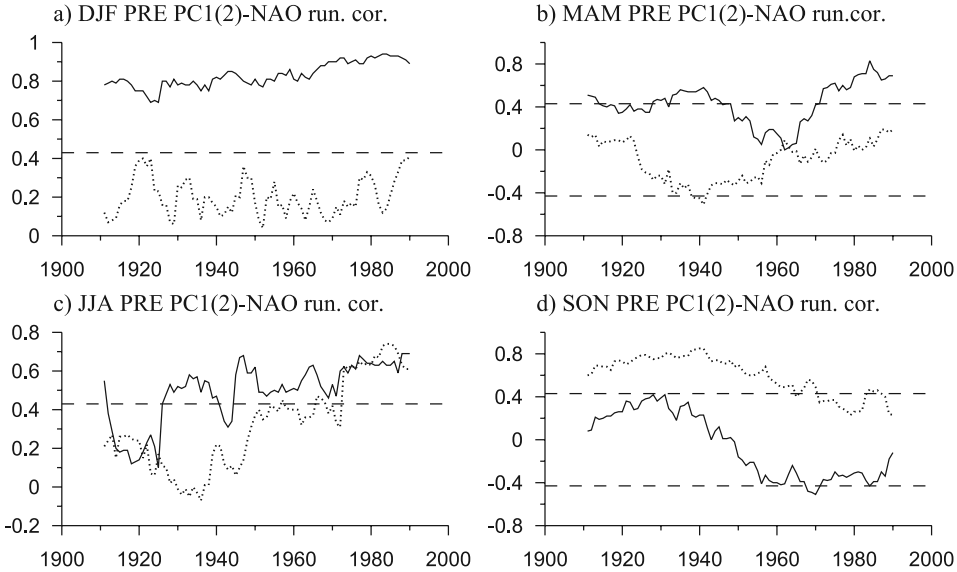

Figure 5. Running correlation coefficients between principal components of the first two EOF modes of the (a) winter, (b) spring, (c) summer, and (d) fall CRU precipitation and the NAO indices calculated over 21-year windows. The first values are plotted in year 11 of the first 21-year period. Solid (dotted) curves depict correlations for PC1 (PC2). Dashed lines indicate 95% significance level.

pattern obtained by *Barnston and Livezey* [1987] from rotated principal component analysis of 700 hPa height anomalies in the Northern Hemisphere. Thus our analysis implies that, in contrast to other seasons characterized by the first EOF modes of precipitation associated with the NAO, the first EOF mode of fall precipitation is linked to the SCA teleconnection pattern.

[30] Correlations between PC of the second EOF mode of fall precipitation and seasonally averaged SON SLP are depicted in Figure 3h. The pattern represents a slightly shifted eastward "classic" NAO pattern (i.e., meridional dipole). The largest negative correlations are detected over Scandinavia (−0.7), whereas the largest positive correlations (0.5) are found over the Iberian Peninsula. Correlation between the PC2 and the fall NAO index is rather high (0.57) and statistically significant at the 99% confidence level according to Student's *t* test [*Bendat and Piersol*, 1966]. We note that this correlation is larger than those obtained for the NAO-associated modes of spring and summer precipitation. Thus correlation analysis suggests that the second EOF mode of fall precipitation over Europe is associated with the NAO.

[31] To verify results of the above correlation analysis with SLP fields, we estimated in a similar manner correlations between PCs of the leading modes of seasonal mean precipitation and seasonally averaged 500 hPa fields from the NCEP/NCAR reanalysis for 1951–2000. Results of this correlation analysis are shown in Figure 4, where positive (negative) correlations are depicted by solid (dashed) curves, and significance level exceeding 95% is indicated by shading.

[32] In general the correlation patterns in Figure 4 are in a good agreement with those shown in Figure 3. The major action centers, earlier detected in SLP fields, are revealed also in 500 hPa fields. Also several additional relatively weak action centers are seen in 500 hPa fields (e.g., correlation patterns for the fall season). It is worth noting, that correlations in Figure 4 are generally larger than those in Figure 3. There are two major reasons for these larger correlations. First, low-frequency atmospheric variability is better pronounced in the middle troposphere. Second, during recent decades the NAO index demonstrated an evident upward trend [e.g., *Hurrell*, 1995], reflecting strengthening of the NAO. Therefore correlations with 500 hPa fields estimated for 1951–2000 are generally larger than correlations with SLP estimated for 1901–2000. Minor differences between correlation patterns obtained for SLP (Figure 3) and 500 hPa (Figure 4) might be attributed to different climatic variables, time periods analyzed, and spatial resolution of the two data sets (5° latitude by 10° longitude grid for SLP and 2.5° latitude by 2.5° longitude grid for 500 hPa).

4.2. Running Correlations Between Leading PCs and the NAO Index

[33] Considered in the previous section correlations to the major regional climate signal, the NAO have been studied in more detail by expanding the overall correlations (estimated for the entire 20th century) into running correlations, on the basis of 21-year overlapping periods between leading PCs of seasonal precipitation and respective (i.e., estimated for each season) indices of the NAO. The estimated running correlations are shown in Figure 5.

[34] In winter (Figure 5a) correlations between PC1 of precipitation and the NAO index are very high and statistically significant during the entire 20th century. They show an evident upward trend persisting from the beginning to the end of the century, and reflecting long-term strengthening of the links between DJF precipitation over Europe and the NAO. Interannual variations of these correlations are relatively weak. On the contrary, correlations between PC2 of DJF precipitation and the NAO demonstrate large interannual variations, but there is no trend (Figure 5a). Moreover, during

the entire century these correlations are not statistically significant.

[35] Running correlations between PC1 of spring precipitation and the NAO index depict phases of relatively high and low correlations (Figure 5b). In particular, from late 1940s to the late 1960s correlations are low (dropping almost to zero in early 1960s) and statistically insignificant, whereas statistically significant and relatively high correlations (reaching 0.8 in the early 1980s) are detected before and after that period. Thus, in contrast to the winter season, strength of the links between spring precipitation and the NAO changed significantly during the 20th century. These interdecadal changes explain why the correlation to the NAO index estimated for the entire 20th century (0.41) is significantly lower than that obtained for the winter season (0.85). Similar interdecadal changes (but with opposite sign) are evident in running correlations between PC2 of MAM precipitation and the NAO index (Figure 5b). However, like in the winter season these correlations in general are not statistically significant.

[36] During summer, correlations between PC1 of precipitation and the NAO index are low and statistically insignificant at the beginning of the 20th century (Figure 5c). Starting from the late 1920s these correlations are relatively high and mostly significant. Their temporal evolution reveals both upward trend and large interannual variations. Running correlations between PC2 of JJA precipitation and the NAO index are statistically significant only during the most recent decades (Figure 5c). In general temporal behavior of these correlations looks like random fluctuations.

[37] Correlations between PC1 of fall precipitation and the NAO index are not statistically significant during almost the entire 20th century (Figure 5d). Marginally significant negative correlations are detected only in late 1960s. This result is somewhat expected because earlier we have shown that this mode is associated with the SCA teleconnection pattern. PC2 of the SON precipitation is significantly correlated with the NAO index from the beginning of the century until 1970s (the largest correlations, reaching 0.85, are detected in late 1930s to early 1940s), and the correlations are generally insignificant during recent decades (Figure 5d).

[38] Two major conclusions can be drawn from the analysis of running correlations. First, in all seasons, the strength of the links between European precipitation and the NAO varied significantly during the 20th century, thus implying essential nonstationarity of these links. Second, evident seasonality is revealed in the long-term variations of the above links. For example, temporal evolution of the winter correlations is characterized by the upward trend (Figure 5a), whereas major feature of the spring correlations is quasiperiodic interdecadal variations (Figure 5b). Indeed, there are no two seasons characterized by similar long-term variations of links between precipitation and the NAO.

[39] Correlation analysis performed in this section revealed links between European precipitation and major regional modes of atmospheric circulation. Some of the established links are consistent with earlier findings (e.g., wintertime links to the NAO), while the others are revealed for the first time (e.g., link to the SCA teleconnection pattern during fall). It is worth mentioning, that while correlations between principal components and indices of teleconnection patterns (except the NAO) were estimated for the second half of the century (i.e., the period for which the indices are available), the correlation analysis with SLP fields is performed on the 100-year time series covering the entire 20th century. Moreover, this analysis provides dynamical context for the leading modes of precipitation that are not associated with the known teleconnection patterns. Major results of this analysis are confirmed by the analysis of correlations with 500 hPa fields for 1951–2000. Analysis of running correlations revealed essential nonstationarity of the links between European precipitation and the NAO. Also significant seasonality has been revealed in the long-term variations of these links.

5. Summary and Discussion

[40] In the present study we analyzed the long-term climatic variability of precipitation over Europe on the basis of data from the CRU data set [*New et al.*, 1999, 2000; *Mitchell and Jones*, 2005] for 1901–2000. Special emphasis was made on the seasonality of long-term precipitation variations. Essential seasonality has been revealed both in spatial-temporal structure of European precipitation variability and in its links to atmospheric circulation.

[41] The leading EOF modes of seasonal mean precipitation are clearly season-dependent. The first EOF modes of the winter, spring and summer precipitation are all associated with the NAO. However, the spatial-temporal structure of the first EOF mode of the summer precipitation differs significantly from those of the winter and spring precipitation. As we earlier noted [*Zveryaev*, 2004], the first EOF mode of the summer precipitation features longer (compared to the respective winter mode) decadal-interdecadal variations, which are consistent with those detected in sea level pressure over the northeast Atlantic by *Hurrell and Folland* [2002]. These long-term variations of European summer precipitation might be associated with the Atlantic Multidecadal Oscillation (AMO) [*Delworth and Mann*, 2000; *Kerr*, 2000]. Recently *Sutton and Hodson* [2005] provided evidence that during the 20th century the AMO had an important role in modulating boreal summer climate on multidecadal timescales. It is worth noting that besides differing structure of the atmospheric circulation that affects summer precipitation variability, the other factor that also plays an important role is land surface processes. For example, *Koster and Suarez* [1995] analyzing model simulations found that the land's contribution to the precipitation variance is strongest during summer, probably because of the response of moist convective processes to land fluxes. Moist convection occurs when atmospheric lapse rates are unstable, and it can be triggered by moisture and heat fluxes at the surface. Through variations in evaporation rate, the land surface can strongly influence variations in moist convective precipitation. Recent studies [*Trenberth*, 1999; *Trenberth et al.*, 2003] show that the recycling ratio varies significantly from lower values in winter to higher values in summer, when the large-scale moisture transport is diminished in importance.

[42] It is shown for the first time that the first EOF mode of the fall precipitation is not associated with the NAO. Our analysis revealed strong and statistically significant link of this mode of precipitation to the SCA teleconnection pattern. The SCA teleconnection pattern is a prominent mode of low-frequency variability present in all months except June and

July, and has been previously referred to as Eurasia-1 pattern by *Barnston and Livezey* [1987].

[43] The second EOF modes of precipitation during different seasons are associated with the different teleconnection patterns. Consistent with analysis of CMAP precipitation for the shorter period [*Zveryaev*, 2004], the second EOF mode of winter CRU precipitation is linked to the EA teleconnection pattern [*Barnston and Livezey*, 1987]. Our analysis has shown that the second EOF mode of fall precipitation is associated with the NAO. Links between the second EOF modes of spring and summer precipitation and regional teleconnection patterns were not found. However, correlations between respective principal components and SLP and 500 hPa fields form the patterns (Figures 3d, 3f, 3d, and 3f) structurally similar to the NAO pattern, but significantly shifted southeastward in case of the spring mode of precipitation, and northeastward in case of the summer mode. Nevertheless, further analysis is needed in order to reveal physical mechanisms forming these modes of precipitation variability.

[44] Analyzing running correlations, we revealed nonstationarity in the links between the leading modes of European precipitation and the NAO. Indeed, this result is not so surprising. Recently *Touchan et al.* [2005] found nonstationary relationships between major modes of European atmospheric circulation and late spring/summer precipitation over eastern Mediterranean. Also, through analysis of running correlations, *Pauling et al.* [2006] detected essential nonstationarities in the relationships between large-scale atmospheric circulation and regional precipitation over southern Spain/northern Morocco and central Europe during winter. However, the present study considers for the first time nonstationarities of the links between continental-scale (for Europe) variations of precipitation and the leading regional mode of atmospheric circulation (the NAO), as well as seasonality of these nonstationarities. Taking into account seasonal differences of the revealed nonstationarities, it is difficult at this stage to propose mechanisms, explaining these nonstationaities. However, wintertime trend-like strengthening of the links (Figure 5a) might be associated with the global warming. Because global warming is better pronounced during winter season and because it is stronger in higher and weaker in lower latitudes [e.g., *Briffa and Osborn*, 2002; *Jones et al.*, 2003], it can be speculated that associated changes in the pressure fields result in increase of the meridional pressure gradient, that eventually leads to enhanced atmospheric moisture transport and increased precipitation over Europe. During summer interdecadal changes in the links to the NAO might be associated with the above mentioned Atlantic Multidecadal Oscillation. However, further investigation of this possible association is necessary.

[45] In the present study we explored the key features of seasonality in long-term variability of precipitation over Europe. We found that the leading EOF modes of European precipitation demonstrate pronounced seasonal differences. Character of their links to atmospheric circulation is also season-dependent. Moreover, analysis of running correlations revealed essential nonstationarity of the links between the leading modes of European precipitation and the NAO. This makes further improvement of seasonal prediction of regional precipitation even more complicated. Further diagnostic studies of the observational data as well as model experiments will provide useful information for the seasonal climate prediction for the European region. Note, however, that detected features of precipitation variability and its links to atmospheric circulation should be periodically revised and updated because they are a subject to long-term changes. The findings of the present study imply that further analysis of seasonality in regional climate variability is necessary.

[46] **Acknowledgments.** The author thanks Marina Goncharova and Richard Allan for their reading and careful editing of the manuscript. This research was supported by the Russian Foundation for Basic Research grant 05-05-64908 and by the NATO under the NATO-SfP-981044 project. The CRU TS 2.0 data has been supplied by the Climate Impacts LINK Project (U.K. Department of the Environment Contract EPG 1/1//16) on behalf of the Climatic Research Unit, University of East Anglia. The manuscript was significantly improved by the constructive comments of anonymous reviewers.

References

Barnston, A. G., and R. E. Livezey (1987), Classification, seasonality and persistence of low-frequency atmospheric circulation patterns, *Mon. Weather Rev.*, *115*, 1083–1126.

Basnett, T. A., and D. E. Parker (1997), Development of the global mean sea level pressure data set GMSLP2', *Clim. Res. Tech. Note 79,* Met Off., Bracknell, U. K.

Bendat, J. S., and A. G. Piersol (1966), *Measurement and Analysis of Random Data*, 390 pp., John Wiley, Hoboken, N. J.

Bretherton, C. S., M. Widmann, V. P. Dymnikov, J. M. Wallace, and I. Blade (1999), The effective number of spatial degrees of freedom of a time-varying field, *J. Clim.*, *12*, 1990–2009.

Briffa, K. R., and T. J. Osborn (2002), Blowing hot and cold, *Science*, *295*, 2227–2228.

Cassou, C., and L. Terray (2001), Oceanic forcing of the wintertime low-frequency atmospheric variability in the North Atlantic European sector: A study with the APREGE model, *J. Clim.*, *14*, 4266–4291.

Christensen, J. H., and O. B. Christensen (2003), Severe summertime flooding in Europe, *Nature*, *421*, 805–806.

Colman, A., and M. Davey (1999), Prediction of summer temperature, rainfall and pressure in Europe from preceding winter North Atlantic ocean temperature, *Int. J. Climatol.*, *19*, 513–536.

Corte-Real, J., B. Qian, and H. Xu (1998), Regional climate change in Portugal: Precipitation variability associated with large-scale atmospheric circulation, *Int. J. Climatol.*, *18*, 619–635.

Delworth, T. L., and M. E. Mann (2000), Observed and simulated multidecadal variability in the Northern Hemisphere, *Clim. Dyn.*, *16*, 661–676, doi:10.1007/s003820000075.

Drevillon, M., L. Terray, P. Rogel, and C. Cassou (2001), Mid latitude Atlantic SST influence on European climate variability in the NCEP reanalysis, *Clim. Dyn.*, *18*, 331–344, doi:10.1007/s003820100178.

Hurrell, J. W. (1995), Decadal trends in the North Atlantic Oscillation: Regional temperature and precipitation, *Science*, *269*, 676–679.

Hurrell, J. W., and C. K. Folland (2002), A change in the summer atmospheric circulation over the North Atlantic, *CLIVAR Exch.*, *7*, 52–54.

Jones, P. D., and A. Moberg (2003), Hemispheric and land-scale surface air temperature variations: An extensive revision and an update to 2001, *J. Clim.*, *16*, 206–223.

Jones, P. D., K. R. Briffa, and T. J. Osborn (2003), Changes in the Northern Hemisphere annual cycle: Implications for paleoclimatology?, *J. Geophys. Res.*, *108*(D18), 4588, doi:10.1029/2003JD003695.

Kalnay, E., et al. (1996), The NCEP/NCAR 40-year reanalysis project, *Bull. Am. Meteorol. Soc.*, *77*, 437–471.

Kerr, R. A. (2000), A North Atlantic climate pacemaker for the centuries, *Science*, *288*, 1984–1985.

Koster, R. D., and M. J. Suarez (1995), Relative contributions of land and ocean processes to precipitation variability, *J. Geophys. Res.*, *100*, 13,775–13,790.

Mitchell, T. D., and P. D. Jones (2005), An improved method of constructing a database of monthly climate observations and associated high-resolution grids, *Int. J. Climatol.*, *25*, 693–712.

New, M. G., M. Hulme, and P. D. Jones (1999), Representing twentieth-century space-time climate variability. part I: Development of a 1961–90 mean monthly terrestrial climatology, *J. Clim.*, *12*, 829–856.

New, M. G., M. Hulme, and P. D. Jones (2000), Representing twentieth-century space-time climate variability. part II: Development of a 1901–96 monthly grids of terrestrial surface climate, *J. Clim.*, *13*, 2217–2238.

North, G. R., T. L. Bell, and R. F. Calahan (1982), Sampling errors in the estimation of empirical orthogonal functions, *Mon. Weather Rev.*, *110*, 699–706.

Parker, D. E., P. D. Jones, C. K. Folland, and A. Bevan (1994), Interdecadal changes of surface temperature since the late nineteenth century, *J. Geophys. Res.*, *99*, 14,373–14,399.

Pauling, A., J. Luterbacher, C. Casty, and H. Wanner (2006), Five hundred years of gridded high-resolution precipitation reconstructions over Europe and the connection to large-scale circulation, *Clim. Dyn.*, *26*, doi:10.1007/s00382-005-0090-8.

Portis, D. H., J. E. Walsh, M. El Hamly, and P. J. Lamb (2001), Seasonality of the North Atlantic Oscillation, *J. Clim.*, *14*, 2069–2078.

Qian, B., H. Xu, and J. Corte-Real (2000), Spatial-temporal structures of quasi-periodic oscillations in precipitation over Europe, *Int. J. Climatol.*, *20*, 1583–1598.

Rodwell, M. J., and C. K. Folland (2002), Atlantic air-sea interaction and seasonal predictability, *Q. J. R. Meteorol. Soc.*, *128*, 1413–1443.

Rodwell, M. J., D. P. Rowell, and C. K. Folland (1999), Oceanic forcing of the wintertime North Atlantic Oscillation and European climate, *Nature*, *398*, 320–323.

Shabalova, M. V., and S. L. Weber (1998), Seasonality of low-frequency variability in early-instrumental European temperatures, *Geophys. Res. Lett.*, *25*, 3859–3862.

Slonosky, V. C., P. D. Jones, and T. D. Davies (2001), Atmospheric circulation and surface temperature in Europe from the 18th century to 1995, *Int. J. Climatol.*, *21*, 63–75.

Sutton, R. T., and D. L. R. Hodson (2005), Atlantic ocean forcing of North American and European summer climate, *Science*, *309*, 115–118.

Touchan, R., E. Xoplaki, G. Funkhouser, J. Luterbacher, M. K. Hughes, N. Erkan, Ü. Akkemik, and J. Stephan (2005), Reconstructions of spring/summer precipitation for the eastern Mediterranean from tree-ring widths and its connection to large-scale atmospheric circulation, *Clim. Dyn.*, *25*, 75–98.

Trenberth, K. E. (1999), Atmospheric moisture recycling: Role of advection and local evaporation, *J. Clim.*, *12*, 1368–1381.

Trenberth, K. E., A. Dai, R. M. Rasmussen, and D. B. Parsons (2003), The changing character of precipitation, *Bull. Am. Meteorol. Soc.*, *84*, 1205–1217.

von Storch, H., and A. Navarra (1995), *Analysis of Climate Variability*, 334 pp., Springer, New York.

von Storch, H., E. Zorita, and U. Cubasch (1993), Downscaling of global climate change estimates to regional scales: An application to Iberian rainfall in wintertime, *J. Clim.*, *6*, 1161–1171.

Wibig, J. (1999), Precipitation in Europe in relation to circulation patterns at the 500 hPa level, *Int. J. Climatol.*, *19*, 253–269.

Wilks, D. S. (1995), *Statistical Methods in the Atmospheric Sciences*, 467 pp., Elsevier, New York.

Xie, P., and P. Arkin (1996), Analyses of global monthly precipitation using gauge observations, satellite estimates, and numerical model predictions, *J. Clim.*, *9*, 840–858.

Xie, P., and P. Arkin (1997), Global precipitation: A 17-year monthly analysis based on gauge observations, satellite estimates, and numerical model outputs, *Bull. Am. Meteorol. Soc.*, *78*, 2539–2558.

Zolina, O., C. Simmer, A. Kapala, and S. Gulev (2005), On the robustness of the estimates of centennial-scale variability in heavy precipitation from station data over Europe, *Geophys. Res. Lett.*, *32*, L14707, doi:10.1029/2005GL023231.

Zorita, E., V. Kharin, and H. von Storch (1992), The atmospheric circulation and sea surface temperature in the North Atlantic area in winter: Their interaction and relevance for Iberian precipitation, *J. Clim.*, *5*, 1097–1108.

Zveryaev, I. I. (1999), Decadal and longer changes of the winter sea level pressure fields and related synoptic activity over the North Atlantic, *Int. J. Climatol.*, *19*, 1177–1185.

Zveryaev, I. I. (2004), Seasonality in precipitation variability over Europe, *J. Geophys. Res.*, *109*, D05103, doi:10.1029/2003JD003668.

I. I. Zveryaev, P. P. Shirshov Institute of Oceanology, RAS, 36, Nakhimovsky Ave., Moscow, 117997, Russia. (igorz@sail.msk.ru)